

⁷R. E. McDonald, to be published.

⁸R. A. Chalmers, to be published; L. F. Chase, Jr., in *Nuclear Research with Low Energy Accelerators*, edited by J. B. Marion and D. M. Van Potter (Academic Press, Inc., New York, 1967), p.445

⁹S. Hinds, J. H. Bjerregaard, Ole Hansen, and O. Nathan, *Phys. Letters* **21**, 328 (1966); D. C. Williams, J. D. Knight, and W. T. Leland, *Phys. Letters* **22**, 162 (1966).

¹⁰M. Soga, private communication.

PROMPT NEUTRONS FROM FISSION OF U^{238} INDUCED BY 12-MeV PROTONS

Eli Cheifetz and Zeev Fraenkel

Department of Nuclear Physics, Weizmann Institute of Science, Rehovot, Israel

(Received 8 April 1968)

The number of prompt neutrons and their average energies in correlation with fragment mass and kinetic energy have been measured directly for fission induced in U^{238} by 12-MeV protons. The sawtooth behavior evident for the average number of neutrons as a function of fragment mass (similar to the behavior in thermal neutron fission of U^{233} , U^{235} , and Pu^{239}) disappears for events of low total kinetic energy.

Until now information about neutrons from medium-excitation fission in correlation with the mass of the fragments has been obtained indirectly by comparing "initial mass distribution" (i.e., mass distribution before neutron emission as deduced from fragments' velocity measurements) with "final mass distribution" (deduced from kinetic energy measurements or radiochemical yields). Britt and Whetstone¹ and Whetstone² bombarded Th^{230} , Th^{232} , and U^{233} with alphas of 20.9-25.7 MeV and obtained the average number of neutrons as a function of mass $\bar{\nu}(A)$ which showed only a slight sawtooth behavior compared with the behavior of neutrons emitted in thermal-neutron fission of U^{235} . Schmitt and Konecny³ used a similar technique to study neutrons from fission of Ra^{226} induced by 13-MeV protons and obtained that $\bar{\nu}(A)$ first increases with mass in the symmetric region of mass division and then drops to a minimum at $A = 133$.

In the present experiment, the number and energies of prompt neutrons in correlation with fragment kinetic energies and masses were measured directly for fission caused by the bombardment of U^{238} with 12-MeV protons. The observed $\bar{\nu}(A)$ has a sawtooth behavior similar to that found in low-energy and spontaneous fission for the nuclei in the mass range from U^{233} to Cf^{252} ,⁴ except that the dip in the region of closed-shell masses 128-132 is not as low as the dip in low-energy fission. Observation of $\bar{\nu}$ versus fragment mass for groups of total kinetic energy E_K reveals that for high E_K the sawtooth behavior is very similar to that of low-energy fission and for low E_K there are no minima at closed-shell numbers.

The experimental arrangement of the present experiment is shown in Fig. 1. The fragments were measured by two pairs of solid-state detectors placed at 45° and 135° to the beam direction. The detectors at 135° were placed 8.0 cm from the target, whereas the detectors at 45° were 5.0 cm from the target. Close to 100% efficiency in counting both fragments was obtained with respect to the detectors at 8.0 cm. A target of $100\text{-}\mu\text{g}/\text{cm}^2$ natural uranium (UO_2 on $30\text{-}\mu\text{g}/\text{cm}^2$ carbon backing) was placed in an average beam of $0.15\text{-}\mu\text{A}$ current inside a cylindrical aluminum chamber of 30-cm diam and 16-cm height. The wall thickness of the chamber was 0.5 cm. The neutrons were detected at a distance of 70 cm from the target by two NE102A plastic scintilla-

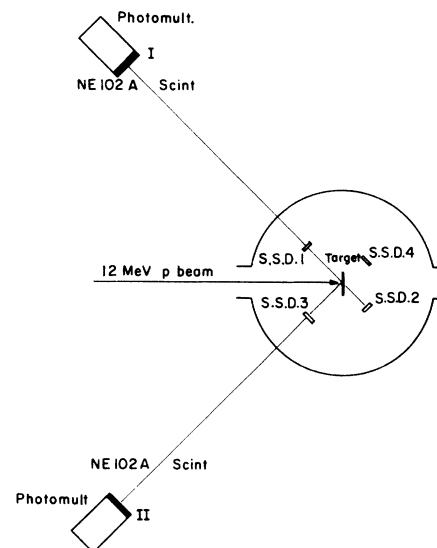


FIG. 1. Experimental arrangement. S.S.D. denotes the solid state detector.

tors of 12.5-cm diam and 5-cm thickness mounted on 58AVP photomultipliers at 135° to the beam. The neutron energies were measured by a time-of-flight technique. The start pulse was given by solid-state detectors at 135° via time pick-off units, and the stop pulse was given by the photomultiplier anode. The kinetic energies of the two fragments and the neutron time of flight were recorded simultaneously by a Nuclear Data, Inc., four-dimensional analyzer. Random time-of-flight events were recorded and given distinct identity. An identical experiment, but one using a thin Cf^{252} source instead of the U^{238} target, served both for the fission-fragment energy calibration using the Schmitt mass-dependent procedure⁵ and for the neutron-detector efficiency determination. The neutron time-of-flight spectrum derived from the Cf^{252} source was compared with the results of Bowman, Thompson, Milton, and Swiatecki⁶ and an "effective" efficiency extracted. Effects such as time-resolution dispersion and scattering or absorption of neutrons in the walls of the chamber appear in the measurements of both Cf^{252} and U^{238} neutrons. Since the neutron spectra of both sources are similar in shape, the use of an "effective" efficiency corrects for the above-mentioned effects to a first order.

The analysis of the results is complicated by the fact that the observed neutron spectrum at each angle to the fission direction is composed of prefission and postfission neutrons. The method used in the analysis was developed previously for treatment of prompt neutrons from high-excitation fission and will be described in detail elsewhere.⁷ A short summary follows.

The two basic assumptions are the following:

(a) Prefission neutrons are not correlated with the fission-fragment direction but may be correlated with the beam axis; therefore, prefission neutrons are isotropic when measured in an azimuthal direction to the beam.

(b) Postfission neutrons are emitted isotropically in the center of mass of the fully accelerated fragments.

On the basis of these assumptions an iteration procedure is used (all angles to be discussed below are defined with respect to the fission-fragment direction). The iteration procedure begins by assuming all neutrons at 0° to be postfission. The neutron spectrum at 0° is transformed to the fragment c.m. system. Evaluated in the c.m. system, its contribution to 90° in the laboratory system can be deduced (the contribution of the

complementary fragment being added) and subtracted from the measured spectrum at 90° , thus resulting in an estimated prefission neutron spectrum. This prefission neutron spectrum is then subtracted from the 0° neutron spectrum yielding a corrected postfission neutron spectrum at 0° . This spectrum, in turn, is transformed again to the fragment c.m. system from which the average number of neutrons and their average c.m. energies are calculated. A correction is made for neutrons contributed by the other fragment; the magnitude of this correction is small.

In practice, the events were analyzed by sorting neutron events into 280 "boxes" representing different regions of fragment masses and total kinetic energies. The neutron time-of-flight spectrum, the yield of binary fission, and the average fragment velocity were found for each "box." The standard deviation for the velocity in each "box" was typically less than 1% of the average velocity. Random events were subtracted from each neutron spectrum by subtracting the average total random events per channel multiplied by the fractional fission yield of each "box." The laboratory spectra were then ready for the necessary iterations. The neutron spectrum of the complementary fragment was the spectrum associated with a "box" of same E_K and complementary mass. The dispersion in mass was mainly due to the target thickness and is estimated to have standard deviation of 2.5 amu.

The total number of postfission neutrons deduced from the 0° neutron spectrum and corrected for prefission neutrons is 3.86 ± 0.18 . Without prefission correction (i.e., assuming that all the observed neutrons at 0° are postfission) the result is 4.47 ± 0.15 . The errors quoted above reflect the difference of the results obtained from the two independent neutron detectors in addition to the statistical errors. The number of prefission neutrons, defined in this text, consists of all neutrons assumed to be emitted isotropically in the laboratory. It included spallation and "scission" neutrons. Spallation neutrons are the neutrons evaporated from the compound nucleus in competition with fission; "scission" neutrons are defined as neutrons emitted isotropically in the laboratory in the process of fission and have been postulated in order to explain the angular distribution of prompt neutrons from Cf^{252} spontaneous fission.⁶ Using the above-described iteration procedure to study "prefission" neutrons in

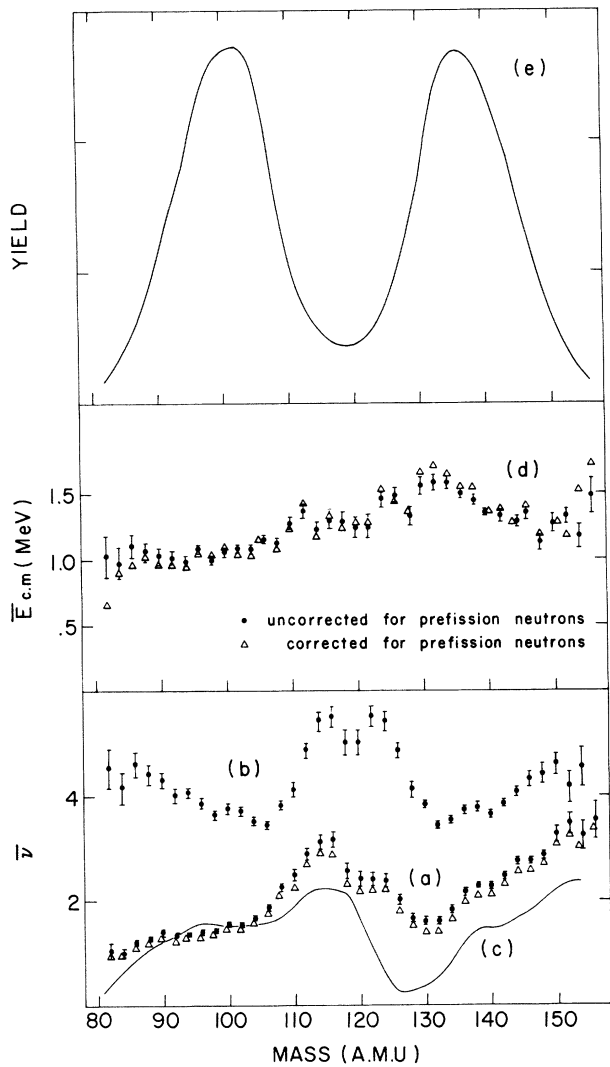


FIG. 2. (a) Average number of neutrons per fragment as a function of mass. Dot, not corrected for pre-fission neutrons. Δ , corrected for pre-fission neutrons. (b) Total number of neutrons as a function of mass division. (c) Average number of neutrons per fragment for fission of $\text{Pu}^{239} + n_{th}$, reproduced from Fraser and Milton (Ref. 9). (d) Average neutron c.m. energy as a function of mass. (e) Mass yield of fission fragments.

Cf^{252} , we found that 0.25 ± 0.20 neutrons are emitted isotropically in the laboratory system. In the U^{238} experiment 0.62 ± 0.25 pre-fission neutrons with velocity above 1.0 cm/nsec were found. The large error stated for these last numbers derives from the considerable uncertainty in efficiency for neutron velocities in the region 1.0-1.5 cm/nsec, as in this region the effects of scattering from the chamber walls are important (the effect on postfission neutrons is smaller because the transformation from labora-

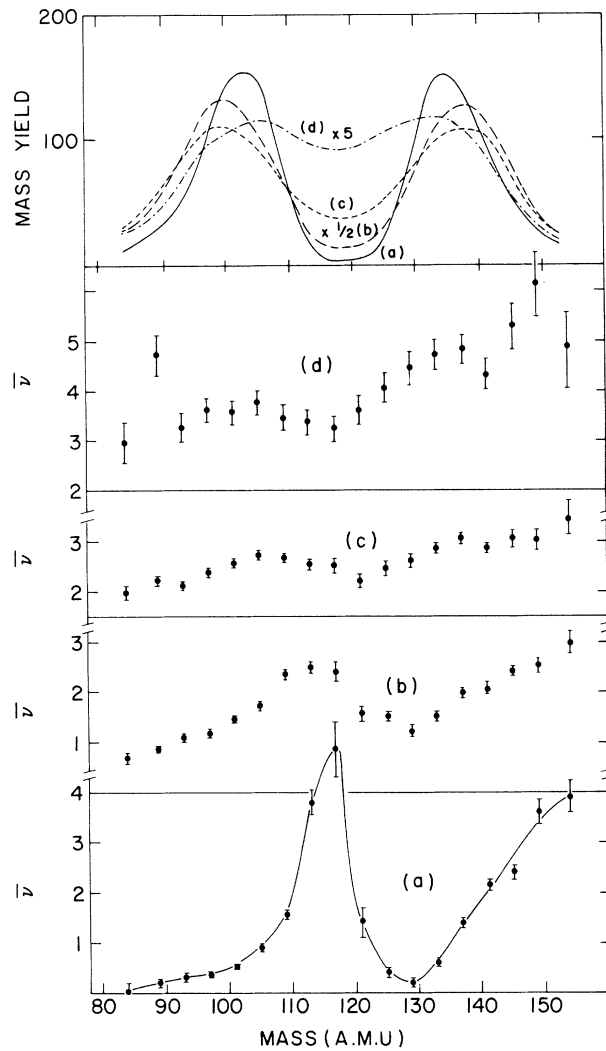


FIG. 3. Average number of neutrons per fragment versus mass for groups of "reduced"-kinetic-energy intervals (a) 206-186 MeV, (b) 186-172 MeV, (c) 172-160 MeV, (d) 160-148 MeV. The mass yield associated with the groups is shown in the upper part.

tory to the fragment c.m. system attaches a low weight to events in this region). On the basis of fission-spallation competition calculations and measurements for Np^{239} ,⁸ 0.25-0.42 spallation neutrons are expected before fission. This number, with the addition of the "scission" neutrons, must be compared with our experimental results.

Figure 2 shows the dependence of the average number of postfission neutrons $\bar{\nu}$ and of their average c.m. energy on the fragment mass corrected for neutron emission. The results are shown with and without correction for pre-fission neutrons; it is evident that the correction for pre-fis-

sion neutrons has little effect on the shape of the distribution. Fine details in the behavior of $\bar{\nu}(A)$ may be obscured by the dispersion in mass. The result of $\bar{\nu}(A)$ for $\text{Pu}^{239} + n_{\text{th}}^9$ is shown for comparison with the U^{238} results. The fissioning nuclei are similar and the difference in the two curves is presumably mainly due to the difference in excitation energy. The difference in $\bar{\nu}(A)$ seems to be much larger for the heavy fragments than for the light fragments.

Figure 3 shows $\bar{\nu}(A)$ plotted for groups of "reduced" total kinetic energies \bar{E}_K defined by $\bar{E}_K = E_K(239/2)^2/(239-A)A$. $\bar{\nu}(A)$ is shown for groups of "reduced" total kinetic energy \bar{E}_K rather than the uncorrected kinetic energy E_K in order to eliminate to a first approximation the effect of the charge division (as correlated with the mass division) on the variation of the total kinetic energy. Britt, Wegner, and Gursky¹⁰ have found that in medium-excitation fission the average \bar{E}_K (they use a parameter called "scission distance" which is inversely proportional to \bar{E}_K) is lower for events in the symmetric mass region than for events in the asymmetric region and have suggested that the symmetric fission events appearing in medium-excitation fission are due to a second "fission mode" not influenced by shell structure of the fragments and occurring with increasing yield as the excitation energy increases.

The graph for high values of \bar{E}_K [Fig. 3(a)] shows very strong variations in number of neu-

trons as a function of mass and very asymmetric mass distribution, whereas the sawtooth behavior becomes less pronounced as \bar{E}_K decreases and the symmetric mass yield increases [Figs. 3(b) and 3(c)]. For very low \bar{E}_K there is no minimum of $\bar{\nu}(A)$ at $A = 130$; this function increases smoothly in the symmetric mass region between $A = 115$ and $A = 140$ as also observed by Schmitt and Konecny³ in the symmetric mass region of Ra^{226} .

¹H. C. Britt and S. I. Whetstone, Jr., Phys. Rev. **133**, B603 (1964).

²S. L. Whetstone, Jr., Phys. Rev. **133**, B613 (1964).

³H. W. Schmitt and E. Konecny, Phys. Rev. Letters **16**, 1008 (1966).

⁴J. Terrell, in Proceedings of the International Symposium on the Physics and Chemistry of Fission, Salzburg, 1965 (International Atomic Energy Agency, Vienna, Austria, 1965), Vol. II, p. 3.

⁵H. W. Schmitt, W. E. Kiker, and C. W. Williams, Phys. Rev. **137**, B837 (1965).

⁶H. R. Bowman, S. G. Thompson, J. C. D. Milton, and W. J. Swiatecki, Phys. Rev. **126**, 2120 (1962).

⁷J. Peter, E. Cheifetz, Z. Fraenkel, M. Lefort, and X. Tarrago, to be published.

⁸R. Vandenbosch and J. R. Huizenga, in Proceedings of the Second United Nations International Conference on the Peaceful Uses of Atomic Energy (United Nations, Geneva, Switzerland, 1958), Vol. 15, p. 284.

⁹J. S. Fraser and J. C. D. Milton, Ann. Rev. Nucl. Sci. **16**, 379 (1966).

¹⁰H. C. Britt, H. E. Wegner, and J. C. Gursky, Phys. Rev. **129**, 2239 (1963).

STRUCTURE OF $\text{O}^{16\dagger}$

A. P. Zuker and B. Buck

Brookhaven National Laboratory, Upton, New York

and

J. B. McGrory

Oak Ridge National Laboratory, Oak Ridge, Tennessee*

(Received 27 May 1968)

An exact shell-model calculation is presented that gives a good description of the properties of O^{16} and neighboring nuclei.

We wish to present a model which gives a good description of the energy spectra of O^{16} and neighboring nuclei. An outstanding property of O^{16} is the coexistence of low-lying states with so widely divergent characteristics that they have hitherto been described by unrelated models, e.g., developments of the spherical shell model using the particle-hole picture for negative parities¹ and

deformed basis calculations for the rotational band beginning at 6 MeV.²⁻⁴ The new feature of the present approach is to give a unified account of the coexisting states within the framework of an exact shell-model calculation.⁵ The basis we selected includes all possible states of four particles moving in the $1p_{1/2}$, $2s_{1/2}$, and $1d_{5/2}$ orbitals. The $1p_{3/2}$ and $1d_{3/2}$ levels were ignored in